

Synthesis, Magnetism, and Crystal Structure of $\text{Li}_2\text{Fe}[(\text{PO}_4)(\text{HPO}_4)]$ and its Hydrogen Position Refinement

Jin-Xiao Mi^a, Horst Borrmann^b, Hui Zhang^b, Ya-Xi Huang^b, Walter Schnelle^b, Jing-Tai Zhao^{*c} and Rüdiger Kniep^b

^a Xiamen/P. R. China, Xiamen University, College of Chemistry and Chemical Engineering

^b Dresden/Germany, Max-Planck-Institut für Chemische Physik fester Stoffe

^c Shanghai/P. R. China, State Key Laboratory of High Performance Ceramics and Superfine Microstructure, Shanghai Institute of Ceramics, Chinese Academy of Sciences

Received August 18th, 2003; revised June 2nd, 2004.

Abstract. Lithium iron(III) monophosphate-monohydrogen-monophosphate, $\text{Li}_2\text{Fe}[(\text{PO}_4)(\text{HPO}_4)]$, was synthesized under mild hydrothermal conditions and its crystal structure was determined by single crystal X-ray diffraction methods. Crystallographic data: monoclinic, $P12_1/n1$ (no. 14), $a = 4.8142(2) \text{ \AA}$, $b = 7.9898(4) \text{ \AA}$, $c = 7.4868(4) \text{ \AA}$, $\beta = 104.398(3)^\circ$, $V = 278.93(2) \text{ \AA}^3$, $Z = 2$, $D_x = 3.104 \text{ g} \cdot \text{cm}^{-3}$. The structure is characterized by FeO_6 octahedra sharing common O-corners with six neighbouring PO_4 tetrahedra to form a three-dimensional framework. Lithium cations are located within channels running along [100]. The channels are

formed by eight-membered rings resulting from the connection of alternating FeO_6 octahedra ($4\times$) and phosphate tetrahedra ($4\times$). High-resolution diffraction data allowed to refine a split model for the position of the hydrogen atom. Magnetization data confirm the valence state $3+$ for iron and detect an antiferromagnetic ordering of the iron moments below 23.6 K. Thermal decomposition of the compound was investigated by DTA/TG methods.

Keywords: Hydrogen disorder; Iron phosphate; Hydrothermal synthesis; Crystal structure; Magnetic properties

Synthese, Magnetismus und Kristallstruktur von $\text{Li}_2\text{Fe}[(\text{PO}_4)(\text{HPO}_4)]$ mit Verfeinerung der Position des Wasserstoffatoms

Inhaltsübersicht. Lithium-Eisen(III)-monophosphat-monohydrogenphosphat, $\text{Li}_2\text{Fe}[(\text{PO}_4)(\text{HPO}_4)]$, wurde unter milden hydrothermalen Bedingungen dargestellt und die Kristallstruktur durch Röntgenbeugung am Einkristall bestimmt. Kristallographische Daten: monoklin, $P12_1/n1$ (Nr. 14), $a = 4,8142(2) \text{ \AA}$, $b = 7,9898(4) \text{ \AA}$, $c = 7,4868(4) \text{ \AA}$, $\beta = 104,398(3)^\circ$, $V = 278,93(2) \text{ \AA}^3$, $Z = 2$, $D_x = 3,104 \text{ g} \cdot \text{cm}^{-3}$. Die Struktur ist durch FeO_6 -Koordinationsoktaeder charakterisiert, die über gemeinsame Ecken mit sechs benachbarten PO_4 -Tetraedern zu einem dreidimensionalen Netzwerk verknüpft sind. Die Lithium-Kationen befinden sich in entlang [100]

verlaufenden Kanälen. Der Durchmesser der Kanäle wird durch achtgliedrige Ringe bestimmt, die aus der alternierenden Verknüpfung von FeO_6 -Oktaedern ($4x$) und PO_4 -Tetraedern ($4x$) resultieren. Die zu hohen Beugungswinkeln gemessenen Röntgendaten erlauben die Verfeinerung eines Splitmodells für die Position des Wasserstoffatoms. Messungen der magnetischen Suszeptibilität bestätigen die Oxidationsstufe $3+$ für Eisen und zeigen antiferromagnetische Ordnung der Momente des Eisens unterhalb von 23,6 K. Der thermische Abbau der Verbindung wurde mit DTA/TG-Methoden verfolgt.

Introduction

Lithium compounds have attracted the interest of materials scientists as well as chemists due to their potential for applications such as superionic conductors, lithium battery materials, etc. Five different lithium iron phosphates ($\text{LiFe}[\text{PO}_4]$, $\text{LiFe}[\text{P}_2\text{O}_7]$, $\text{LiFe}[\text{P}_3\text{O}_9]$, $\text{Li}_3\text{Fe}_2[\text{PO}_4]_3$, $\text{Li}_9\text{Fe}_3[(\text{P}_2\text{O}_7)_3(\text{PO}_4)_2]$) and two hydrogenphosphates ($\text{LiFe}[(\text{PO}_4)(\text{OH})]$, $\text{LiFe}[(\text{H}_2\text{P}_2\text{O}_7)_2]$) have been reported up to now [1–7]. The new compound $\text{Li}_2\text{Fe}[(\text{PO}_4)(\text{HPO}_4)]$, together with its indium analogue [8], represents a new structure type. In the indium compound, the hydrogen atom position posed an

interesting problem, which had not been solved up to now, i.e. an unambiguous assignment of the anionic units was not possible. Similar situations (order/disorder of hydrogen in hydrogen bridges) have also been encountered in many other phosphate and borophosphate compounds, for example in $(\text{NH}_4)_2\text{In}[\text{P}_2\text{O}_7(\text{OH})]$, $\text{NaGa}[\text{BP}_2\text{O}_7(\text{OH})_3]$, $\text{KGa}[\text{BP}_2\text{O}_7(\text{OH})_3]$, $\text{NaIn}[\text{BP}_2\text{O}_7(\text{OH})_3]$ [9–12], etc. Like in many other hydrogen-bonded systems the local symmetry at the hydrogen atom position caused a symmetric arrangement. The corresponding O–H distances of about 1.2 Å within the symmetric bridges had to be considered as quite unusual.

Experimental

Synthesis

$\text{Li}_2\text{Fe}[(\text{PO}_4)(\text{HPO}_4)]$ was obtained under mild hydrothermal conditions in the course of our investigations on the formation of boro-

* Prof. Dr. Jing-Tai Zhao
Phone: 86((0)21)-5241-2073
Fax: 86((0)21)-5241-3122
e-mail: jtzhao@mail.sic.ac.cn

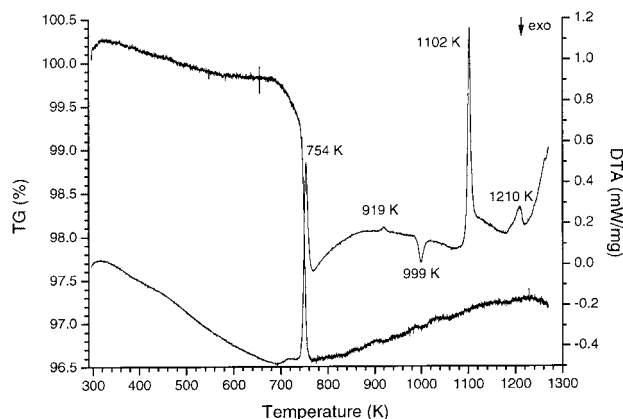


Fig. 1 TG/DTA for $\text{Li}_2\text{Fe}[(\text{PO}_4)(\text{HPO}_4)]$; for further details see text.

phosphates [13]. The reaction was carried out with mixtures of $\text{FeCl}_3 \cdot 6\text{H}_2\text{O}$ (2.703 g), LiH_2PO_4 (5.197 g), and $\text{Li}_2\text{B}_4\text{O}_7$ (1.691 g) with a molar ratio of 1 : 5 : 1 in aqueous solution. The mixture was filled into a 20 ml Teflon autoclave with a filling degree of about 30%. The autoclaves were placed in an oven and kept at 493 K for two weeks. The starting materials were all of analytical grade and were used without further purification. The solid product was washed by hot water and dried in an oven at 340 K. The composition of the product was confirmed by chemical analysis (ICP) with Li 5.36 (calc. 5.33 wt.%), Fe 21.84 (21.42), P 24.55 (23.76) and H 0.415 (0.387). No boron was detected in the product although borate was present during synthesis.

TG/DTA analyses of the title compound (Fig. 1) revealed a strong endothermic peak at 754 K. The corresponding weight loss of about 3.68% is close to the theoretical value of 3.46% for the loss of half a water molecule per formula unit. Obviously, the condensation of hydrogenphosphate groups leads to the release of constitutional water and a mixture of $\text{LiFe}[\text{P}_2\text{O}_7]$ [2] and $\text{Li}_3\text{Fe}_2[\text{PO}_4]_3$ [4] is formed as derived from X-ray powder diffraction patterns. Additional endothermic and exothermic peaks at higher temperatures are presumably corresponding to reactions and melting processes in the phase mixture.

The magnetization of the title compound was measured with a SQUID magnetometer (Quantum Design, MPMS-XL 7) in the temperature range 1.8–320 K. The material showed antiferromagnetic ordering at 23.6(2) K with a weak ferromagnetic component with a magnetization of $0.032 \mu_{\text{B}}$ in 100 Oe external magnetic field (powder average; see Figure 2 bottom). The paramagnetic effective moment μ_{eff} was calculated by non-linear and linear Curie-Weiss fits ($\chi(T) = C/(T-\theta)$) in the range 50–320 K of the $H = 10$ kOe data to $5.97 \mu_{\text{B}}/\text{Fe-atom}$ ($\theta_{\text{p}} = -38.1$ K) and $5.95 \mu_{\text{B}}/\text{Fe-atom}$ ($\theta_{\text{p}} = -37.2$ K), respectively. Commonly found magnetic moments for Fe^{3+} in octahedral coordination are 5.70–6.00 μ_{B} while for Fe^{2+} values of only 5.10–5.70 μ_{B} are observed [14]. The result shows that the material exclusively contains high-spin Fe^{3+} species (see Figure 2 top).

Structure determination

A suitable single crystal of $\text{Li}_2\text{Fe}[(\text{PO}_4)(\text{HPO}_4)]$ (grain, $0.04 \times 0.04 \times 0.06 \text{ mm}^3$) was mounted on a glass fibre with two-

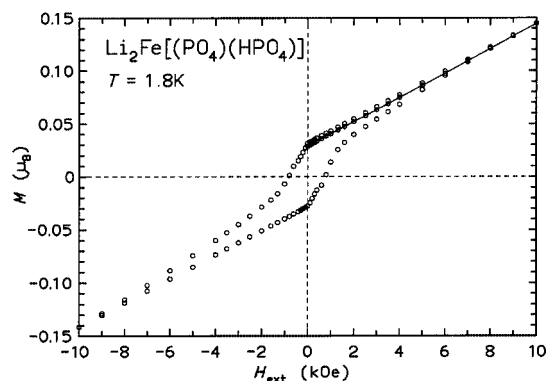
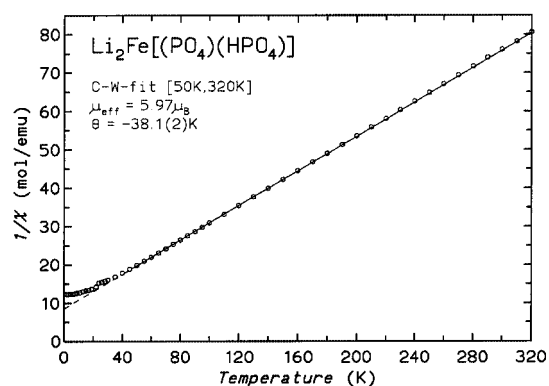


Fig. 2 (top) Inverse magnetic susceptibility of $\text{Li}_2\text{Fe}[(\text{PO}_4)(\text{HPO}_4)]$ in a field of 10 kOe. The line represents the fitted Curie-Weiss law with the parameters μ_{eff} and θ .

(bottom) Isothermal magnetization measurement for $\text{Li}_2\text{Fe}[(\text{PO}_4)(\text{HPO}_4)]$ at 1.8 K.

The symbols connected by a line represent the virgin curve.

component glue. X-ray diffraction data were collected at 295 K using a Rigaku R-axis RAPID diffractometer (graphite monochromator, MoK_α radiation) in the angular range $3.8 \leq \theta \leq 62.5^\circ$. The structure was solved in space group $P12_1/n1$ (no. 14) by direct methods using the program Sir97 [15]. Fourier calculations and subsequent full-matrix least-squares refinements were carried out using SHELXL-97 [16] applying neutral-atom scattering factors. The crystallographic data are summarized in Table 1¹⁾. After anisotropic displacement parameters had been included in the refinement, the hydrogen atom was located in a Fourier difference map and refined using an isotropic displacement parameter. It turned out that the H-atom has to be positioned off the respective center of symmetry. Although the split position is only half occupied, the refinement converged smoothly. A total of 66 variables were refined to $R_1 = 0.055$ and $wR_2 = 0.105$ considering 2953

¹⁾ Further details of the crystal structure investigation are available from the Fachinformationszentrum Karlsruhe, D-76344 Eggenstein-Leopoldshafen (Germany), on quoting the depository number CSD-391239, the name of the authors, and citation of the paper.

Table 1 Crystal data and structure refinement results for $\text{Li}_2\text{Fe}[(\text{PO}_4)(\text{HPO}_4)]$

Crystal size	0.04 × 0.04 × 0.06 mm (pale pink, transparent)
Formula weight / $\text{g} \cdot \text{mol}^{-1}$	260.68
Density calc. / $\text{g} \cdot \text{cm}^{-3}$	3.104
μ ($\text{MoK}\alpha$) / mm^{-1}	3.281
Radiation / Å	$\text{MoK}\alpha$, 0.71073
Measurement temperature	295(2) K
Space group	$P12_1/n1$ (no. 14)
a / Å	4.8142(2)
b / Å	7.9898(4)
c / Å	7.4868(4)
β / °	104.398(3)
Unit cell volume / Å ³	278.93(2)
Z	2
Data measurement method	Rigaku R-axis RAPID diffractometer
	D = 127.40 mm, $2\theta = -143^\circ - 61^\circ$;
	$\chi = 0^\circ$, $\varphi = 0^\circ$, $\omega = 60^\circ - 180^\circ$, $\Delta\omega = 5^\circ$;
	$\chi = 30^\circ$, $\varphi = 90^\circ$, $\omega = 60^\circ - 180^\circ$, $\Delta\omega = 5^\circ$
T_{min} , T_{max}	0.5965, 1.0000
Miller-index-range	$-10 \leq h \leq 11$, $-19 \leq k \leq 19$, $-18 \leq l \leq 18$
θ_{max}	62.67°
Total data collected	12115
Unique data	3879, 2953 ($I > 2\sigma(I)$)
R_{int} , R_{σ}	0.034, 0.030
R_1 [$F^2 > 2\sigma(F^2)$], wR_2 [all]	0.055, 0.105
No. of parameters refined	66
$(\Delta/\sigma)_{\text{max}}$	< 0.001
Goodness-of-fit on F^2	1.097
Residual electron density (min, max) / $\text{e} \cdot \text{Å}^{-3}$	-3.275, 1.396

Table 2 Atomic coordinates, isotropic displacement parameters (Å²) and occupancies for $\text{Li}_2\text{Fe}[(\text{PO}_4)(\text{HPO}_4)]$, e.s.d.'s are given in parentheses

Atoms	Site	x	y	z	$U_{\text{eq}/\text{iso}}$	Occ.
Fe(1)	2b	1/2	1/2	0	0.00534(4)	1
P(1)	4e	0.86814(7)	0.65394(4)	0.73487(4)	0.00503(5)	1
Li(1)	4e	0.3913(7)	0.8653(4)	0.8428(5)	0.0149(5)	1
O(1)	4e	0.6466(2)	0.67604(11)	0.84872(13)	0.00804(12)	1
O(2)	4e	0.9807(2)	0.82247(12)	0.68669(14)	0.00933(13)	1
O(3)	4e	0.1170(2)	0.54604(13)	0.84039(14)	0.00905(13)	1
O(4)	4e	0.7415(2)	0.56006(14)	0.55196(14)	0.01025(14)	1
H(1)	4e	0.571(12)	0.519(9)	0.518(10)	0.020(15)	0.5

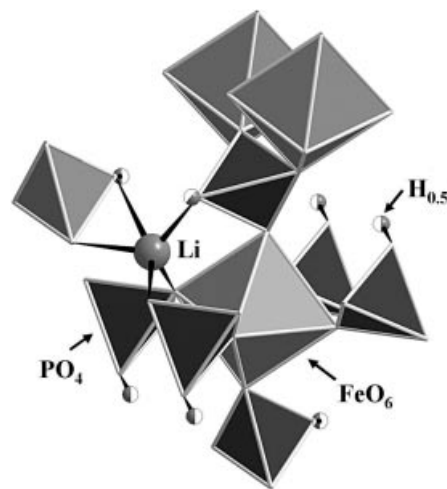
Table 3 Anisotropic displacement parameters (Å²) for $\text{Li}_2\text{Fe}[(\text{PO}_4)(\text{HPO}_4)]$, e.s.d.'s are given in parentheses

Atom	U_{11}	U_{22}	U_{33}	U_{12}	U_{13}	U_{23}
Fe(1)	0.00509(7)	0.00534(6)	0.00545(7)	0.00070(6)	0.00108(6)	0.00030(6)
P(1)	0.00425(10)	0.00545(9)	0.00538(10)	-0.00018(7)	0.00120(8)	0.00070(8)
Li(1)	0.0174(13)	0.0135(12)	0.0149(13)	0.0039(10)	0.0062(10)	0.0028(10)
O(1)	0.0078(3)	0.0078(3)	0.0103(3)	0.0010(2)	0.0054(3)	0.0021(2)
O(2)	0.0109(3)	0.0074(3)	0.0101(3)	-0.0024(2)	0.0035(3)	0.0021(2)
O(3)	0.0061(3)	0.0104(3)	0.0097(3)	0.0026(2)	0.0002(3)	0.0017(3)
O(4)	0.0088(3)	0.0148(4)	0.0068(3)	-0.0045(3)	0.0012(3)	-0.0027(3)

(with $I > 2\sigma(I)$) and 3879 contributing unique reflections, respectively. The atomic positional and displacement parameters, selected interatomic distances, bond angles and bond valence sums are listed in Table 2, Table 3, and Table 4 [17].

Table 4 Selected bond distances, angles and bond valence sums (Σ_s) for $\text{Li}_2\text{Fe}[(\text{PO}_4)(\text{HPO}_4)]$, e.s.d.'s are given in parentheses

Fe(1)–O(3)	1.9667(10) (2x)	Li(1)–O(1)	1.942(3)
Fe(1)–O(2)	2.0096(9) (2x)	Li(1)–O(4)	1.972(3)
Fe(1)–O(1)	2.0389(8) (2x)	Li(1)–O(3)	1.986(3)
$\Sigma_s(\text{Fe}–\text{O}) = 3.095$		Li(1)–O(2)	2.060(4)
P(1)–O(3)	1.5270(10)	Li(1)–O(4)	2.340(4)
P(1)–O(2)	1.5278(9)	$\Sigma_s(\text{Li}–\text{O}) = 1.071$	
P(1)–O(1)	1.5320(9)		
P(1)–O(4)	1.5473(11)	O(2)–P(1)–O(4)	107.64(6)
$\Sigma_s(\text{P}–\text{O}) = 4.840$		O(3)–P(1)–O(2)	109.95(6)
O(4)–H(1)	0.86(5)	O(3)–P(1)–O(4)	105.66(6)
		O(1)–P(1)–O(4)	111.89(6)
O(3)–Fe(1)–O(3)	180	O(3)–P(1)–O(1)	110.02(6)
O(3)–Fe(1)–O(2)	84.72(4)	O(2)–P(1)–O(1)	111.50(5)
O(3)–Fe(1)–O(2)	95.28(4)	O(2)–P(1)–O(4)	147.09(16)
O(2)–Fe(1)–O(2)	180	O(1)–Li(1)–O(4)	124.88(17)
O(3)–Fe(1)–O(1)	86.29(4)	O(1)–Li(1)–O(3)	119.07(16)
O(3)–Fe(1)–O(1)	93.71(4)	O(4)–Li(1)–O(3)	112.33(16)
O(2)–Fe(1)–O(1)	91.04(4)	O(1)–Li(1)–O(2)	113.35(17)
O(2)–Fe(1)–O(1)	88.96(4)	O(4)–Li(1)–O(2)	90.69(14)
O(1)–Fe(1)–O(1)	180	O(3)–Li(1)–O(2)	82.94(13)
P(1)–O(1)–Fe(1)	127.92(5)	O(1)–Li(1)–O(4)	95.13(14)
P(1)–O(2)–Fe(1)	150.08(7)	O(4)–Li(1)–O(4)	85.77(13)
P(1)–O(3)–Fe(1)	156.40(7)	O(3)–Li(1)–O(4)	68.43(11)

**Fig. 3** Main units and respective connectivity in the crystal structure of $\text{Li}_2\text{Fe}[(\text{PO}_4)(\text{HPO}_4)]$.

The position of the hydrogen atom is only half occupied.

Discussion

Structure description

The crystal structure of $\text{Li}_2\text{Fe}[(\text{PO}_4)(\text{HPO}_4)]$ is characterized by FeO_6 octahedra sharing common O-corners with six PO_4 tetrahedra resulting in a three-dimensional framework. Each PO_4 tetrahedron shares common O-corners with three FeO_6 octahedra (see Fig. 3) [18]. According to the split model the hydrogen atom of the terminal OH unit is shared among two PO_4 tetrahedra. The lithium cations reside within quite large channels running along the a -axis and formed by alternating FeO_6 octahedra and phosphate tetrahedra (see Fig. 4 top). The coordination of the Li ion is characterized by four Li–O contacts ranging from 1.942 Å to 2.060 Å to four different PO_4 tetrahedra and one

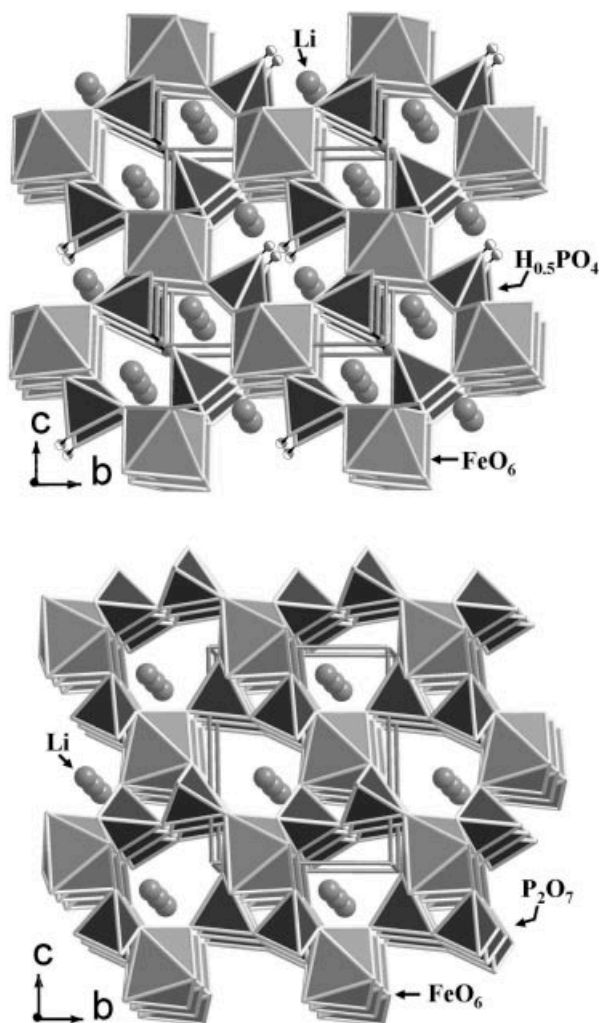


Fig. 4 (top) Crystal structure of $\text{Li}_2\text{Fe}[(\text{PO}_4)(\text{HPO}_4)]$ viewed along [100]. Formal removal of LiOH leads to LiFeP_2O_7 whose structure [2] is depicted at the bottom. See text.

additional contact at 2.340 Å (Fig. 3 and Table 4). The FeO_6 octahedra are arranged about a center of symmetry with $\text{Fe}-\text{O}$ bond distances ranging from 1.967 Å to 2.039 Å. Bond lengths and angles within the PO_4 tetrahedra are well in accordance with respective values in other phosphates [9–12]. An interesting hypothetical relation can be drawn between the structures of $\text{Li}_2\text{Fe}[(\text{PO}_4)(\text{HPO}_4)]$ and LiFeP_2O_7 . Formal removal of one LiOH unit from the title compound results in the composition LiFeP_2O_7 . The loss of the constitutional water gives rise to condensation and formation of $[\text{P}_2\text{O}_7]$ groups. The condensation results in a new arrangement of the building units with the remaining Li ions clearly out of the center of the channels (Fig. 4 bottom).

Hydrogen atom position

In covalently bonded H atoms, a substantial fraction of the electron density is located at the bond region between the

Table 5 Phosphate and borophosphate compounds with a hydrogen atom reportedly located in a special position shared by two oxygen atoms.

Formula	O–H distance (Å)	Reference
$\text{Al}[\text{B}_2\text{P}_2\text{O}_7(\text{OH})_5]\cdot\text{H}_2\text{O}$	1.24	[43]
$\text{Ba}_2\text{Fe}_3\text{H}(\text{PO}_4)_2(\text{P}_2\text{O}_7)_2$	1.20	[22]
$\text{Ba}_2\text{GaH}(\text{P}_2\text{O}_7)_2$	1.27	[23]
$\text{Ba}_2\text{V}_3\text{H}(\text{PO}_4)_2(\text{P}_2\text{O}_7)_2$	1.20	[22]
$\text{CaK}_3\text{H}(\text{PO}_4)_2$	1.24	[24]
$\text{Cs}_2\text{GaH}_3(\text{P}_2\text{O}_7)_2$	1.19	[25]
$\text{CsH}(\text{ZnPO}_4)_2$	1.20	[26]
$\text{CsMnHP}_3\text{O}_{10}$	1.22	[27]
$\text{Cu}_2\text{K}(\text{OH})(\text{PO}_3\text{F})_2\cdot\text{H}_2\text{O}$	1.24	[28]
$\text{Eu}(\text{HP}_2\text{O}_6)(\text{H}_2\text{O})_4$	1.31	[29]
$\text{Fe}(\text{B}_2\text{P}_2\text{O}_7(\text{OH})_5)$	1.32	[30]
$\text{Fe}(\text{NH}_4)\text{HP}_3\text{O}_{10}$	1.20	[31]
$\text{K}_3\text{Cu}_2[(\text{P}_2\text{O}_7)\text{H}(\text{P}_2\text{O}_7)]$	1.20	[32]
$\text{KGa}[\text{BP}_2\text{O}_7(\text{OH})_3]$	1.22	[11]
$\text{KMn}(\text{HP}_3\text{O}_{10})$	1.13, 1.31	[33]
$\text{LnHP}_2\text{O}_6(\text{H}_2\text{O})_4$ (Ln = Gd, Dy, Ho)	1.20	[34]
$\text{MgNa}_3\text{H}(\text{PO}_4)_2$	1.22	[35]
$\text{Na}_5\text{H}_2(\text{PO}_4)(\text{P}_2\text{O}_7)$	1.23	[36]
$\text{NaAl}[\text{BP}_2\text{O}_7(\text{OH})_3]$	1.24	[37]
$\text{NaFe}(\text{BP}_2\text{O}_7(\text{OH})_3)$	1.24	[38]
$\text{NaGa}[\text{BP}_2\text{O}_7(\text{OH})_3]$	1.22	[10]
$\text{Na}_4(\text{HP}_3\text{O}_{10})(\text{H}_2\text{O})$	1.22	[39]
$\text{NaIn}[\text{BP}_2\text{O}_7(\text{OH})_3]$	1.22	[12]
$\text{Nd}(\text{HP}_2\text{O}_6)(\text{H}_2\text{O})_4$	1.31	[40]
$(\text{NH}_4)_2\text{In}(\text{PO}_4)(\text{HPO}_4)$	1.24	[9]
$\text{Pb}_2(\text{Fe}_{0.78}\text{Al}_{0.22})\text{H}(\text{PO}_4)_2(\text{OH})_2$	1.19	[41]
$\text{RbH}_5(\text{PO}_4)_2$	1.22	[42]

Table 6 Difference Fourier peaks after structure refinement on low-angle data including anisotropic displacement parameters for non-hydrogen atoms in $\text{Li}_2\text{Fe}[(\text{PO}_4)(\text{HPO}_4)]$.

	x	y	z	peak	distances to nearest atoms			
Q1	0.5647	0.5209	0.5322	0.48	0.89	O4	1.59	O4
Q2	0.9322	0.7476	0.7107	0.35	0.68	O2	0.85	P1
Q3	0.7877	0.7211	0.8542	0.33	0.76	O1	1.19	P1
Q4	0.7871	0.6036	0.6250	0.32	0.64	O4	0.91	P1
Q5	0.5717	0.5879	0.8776	0.32	0.84	O1	1.27	Fe1
Q6	0.0111	0.5707	0.7992	0.30	0.56	O3	0.99	P1
Q7	0.6778	0.6180	0.5288	0.28	0.56	O4	1.61	P1
Q8	0.2464	0.5598	0.9038	0.26	0.69	O3	1.34	Fe1

atoms. Due to this acentric density distribution, standard least-squares refinements of positional parameters using X-ray data tend to displace hydrogen towards the atom to which it is bonded. Consequently, hydrogen atom positions determined by standard X-ray methods are systematically different from those determined with other methods like neutron diffraction. O–H bond distances from X-ray structure determination are about 0.1–0.2 Å shorter than the internuclear distances [19]. In case of diformohydrazide it had been demonstrated that X-ray data collected to high diffraction angles could offer a way to lift this bias [19, 20]. However, this method was only rarely used. In a considerable number of phosphate containing compounds hydrogen atoms were positioned at centers of symmetry (Table 5). Within these symmetric hydrogen bridges H–O bond distances are typically 1.2–1.3 Å. In many cases it had to be assumed that this model represented an averaged situation

with the H atom at split positions. Only in very rare cases such a model was confirmed on the basis of X-ray diffraction data [21]. For $\text{Li}_2\text{Fe}[(\text{PO}_4)(\text{HPO}_4)]$ we succeeded to obtain high-quality crystals which allowed us to collect diffraction data of excellent quality. After structure refinement on the basis of a data set limited to $2\theta_{\text{max}} = 60^\circ$ the Fourier difference map clearly revealed the position of the hydrogen atom (Table 6). Subsequent refinement of the hydrogen atom including an isotropic displacement parameter confirmed well that a split model at 50 % occupancy on the general position had to be preferred over an ordered model occupying the center of symmetry at $2a$ (0.5, 0.5, 0.5). The latter model would result in O–H distances of 1.24 Å, while the disordered model results in an asymmetric situation with O–H distances of 0.86 Å and 1.62 Å, respectively. Applying various limits with respect to $2\theta_{\text{max}}$ to our data set mainly results in different O–H distances varying between 0.78(5) and 0.86(5) Å. This is in excellent agreement with the experiences of Hope and coworkers [19, 20], however, we did not apply a low-angle cutoff to our data set. This very encouraging result deserves further application of the method to other systems, but also to investigate why the Fourier difference map for the full data set is considerably more noisy.

Acknowledgements. This project was supported by the Fund for Distinguished Young Scholars from the NNSF of China, and Fund of the 863 project from the MOST of China. We are grateful to Dr. R. Niewa and Ms. S. Müller for DTA/TG experiments, and Ms. U. Schmidt for chemical analyses at MPI CPfS in Dresden. JXM and JTZ are indebted to the Max-Planck-Gesellschaft for financial support.

References

- [1] O. V. Yakubovich, M. A. Simonov, N. V. Belov, *Dokl. Akad. Nauk SSSR* **1977**, 235, 93.
- [2] D. Riou, N. Nguyen, R. Benloucif, B. Raveau, *Mat. Res. Bull.* **1990**, 25, 1363.
- [3] E. A. Genkina, B. A. Maksimov, Y. K. Kabalov, O. K. Mel'nikov, *Dokl. Akad. Nauk SSSR* **1983**, 270, 1113.
- [4] A. B. Bykov, A. P. Chirkin, L. N. Demyanets, S. N. Doronin, E. A. Genkina, A. K. Ivanov-Shits, I. P. Kondratyuk, B. A. Maksimov, O. K. Mel'nikov, L. N. Muradyan, V. I. Simonov, V. A. Timofeeva, *Solid State Ionics* **1990**, 38, 31.
- [5] S. Poisson, F. d'Yvoire, N. Guyen-Huy-Dung, E. Bretey, P. Berthet, *J. Solid State Chem.* **1998**, 138, 42.
- [6] E. A. Genkina, Y. K. Kabalov, B. A. Maksimov, O. K. Mel'nikov, *Kristallografiya* **1984**, 29, 50.
- [7] I. Grunze, H. Grunze, *Z. Anorg. Allg. Chem.* **1984**, 512, 39.
- [8] J.-X. Mi, J.-F. Deng, S.-Y. Mao, Y.-X. Huang, H. Borrmann, J.-T. Zhao, R. Kniep, *Z. Kristallogr. NCS*, **2002**, 217, 307.
- [9] M.-R. Li, S.-Y. Mao, H.-H. Chen, J.-F. Deng, J.-X. Mi, J.-T. Zhao, *Z. Kristallogr. NCS* **2002**, 217, 309.
- [10] Y.-X. Huang, S.-Y. Mao, J.-X. Mi, Z.-B. Wei, J.-T. Zhao, R. Kniep, *Z. Kristallogr. NCS* **2001**, 216, 15.
- [11] J.-X. Mi, Y.-X. Huang, S.-Y. Mao, H. Borrmann, J.-T. Zhao, R. Kniep, *Z. Kristallogr. NCS* **2002**, 217, 167.
- [12] Y.-X. Huang, J.-X. Mi, S.-Y. Mao, Z.-B. Wei, J.-T. Zhao, R. Kniep, *Z. Kristallogr. NCS* **2002**, 217, 7.
- [13] R. Kniep, H. Engelhardt, C. Hauf, *Chem. Mater.* **1998**, 10, 2930.
- [14] E. König, G. König in Landolt-Börnstein, New series, Vol. 12/4a, K.-H. Hellwege, A. M. Hellwege (eds.), Springer-Verlag, Berlin 1984.
- [15] A. Altomare, M. C. Burla, M. Camalli, G. Cascarano, C. Giacovazzo, A. Guagliardi, A. G. G. Moliterni, G. Polidori, R. Spagna, *J. Appl. Crystallogr.* **1998**, 32, 115.
- [16] G. M. Sheldrick, SHELXL-97, program for refining crystal structures, University of Göttingen, Germany **1997**.
- [17] N. E. Brese, M. O'Keefe, *Acta Crystallogr.* **1991**, B 47, 192.
- [18] K. Brandenburg, Diamond Version 2.1e, 1996-2001 Crystal Impact GbR, Bonn, Germany.
- [19] J. Almlöf, T. Ottersen, *Acta Crystallogr.* **1979**, A 35, 137.
- [20] H. Hope, T. Ottersen, *Acta Crystallogr.* **1978**, B 34, 3623.
- [21] S. Milicev, A. Rahten, H. Borrmann, J. Šiftar, *J. Raman Spectrosc.* **1997**, 28, 315.
- [22] E. Dvoncova, K.-H. Lii, C.-H. Li, T.-M. Chen, *J. Solid State Chem.*, **1993**, 106, 485.
- [23] K.-F. Hsu, S.-L. Wang, *Acta Crystallogr.* **1999**, C 55, 1400.
- [24] S. Takagi, M. Mathew, W. E. Brown, *Acta Crystallogr.* **1983**, C 39, 166.
- [25] I. Gruntze, S. I. Maksimova, K. K. Palkina, N. T. Chibiskova, N. N. Chudinova, *Izv. Akad. Nauk SSSR, Neorg. Mater.* **1988**, 24, 264.
- [26] T. M. Nenoff, W. T. A. Harrison, T. E. Gier, J. C. Calabrese, G. D. Stucky, *J. Solid State Chem.* **1993**, 107, 285.
- [27] E. V. Murashova, N. N. Chudinova, *Kristallografiya* **1995**, 40, 476.
- [28] F. Moewius, B. Ziemer, G. Reck, M. Meisel, H. Grunze, *Z. Anorg. Allg. Chem.* **1987**, 547, 75.
- [29] V. I. Pakhomov, K. K. Palkina, S. I. Maksimova, N. T. Chibiskova, V. S. Mironova, I. V. Tananaev, *Russ. J. Inorg. Chem.* **1987**, 32, 20.
- [30] I. Boy, C. Hauf, R. Kniep, *Z. Naturforsch.* **1998**, 53 b, 631.
- [31] V. V. Krasnikov, Z. A. Konstant, V. S. Fundamenskii, *Izv. Akad. Nauk SSSR, Neorg. Mater.* **1983**, 19, 1373.
- [32] H. Effenberger, *Acta Crystallogr.* **1987**, C 43, 1237.
- [33] A. J. Wright, C. Ruiz-Valero, J. P. Attfield, *J. Solid State Chem.* **1999**, 145, 479.
- [34] K. K. Palkina, S. I. Maksimova, N. T. Chibiskova, V. S. Mironova, I. V. Tananaev, *Zh. Neorg. Khim.* **1987**, 32, 1790.
- [35] A. Kawahara, J. Yamakawa, T. Yamada, D. Kobashi, *Acta Crystallogr.* **1995**, C 51, 2220.
- [36] D. M. Wiench, M. Jansen, *Acta Crystallogr.* **1983**, C 39, 1613.
- [37] D. Koch, R. Kniep, *Z. Kristallogr. NCS* **1999**, 214, 441.
- [38] I. Boy, G. Cordier, B. Eisenmann, R. Kniep, *Z. Naturforsch.* **1998**, 53 b, 165.
- [39] N. Kindler, M. Jansen, *Z. Anorg. Allg. Chem.* **1997**, 623, 55.
- [40] K. K. Palkina, S. I. Maksimova, N. T. Chibiskova, *Zh. Neorg. Khim.* **1983**, 28, 885.
- [41] G. S. D. King, L. Sengier Roberts, *Bulletin de Mineralogie* **1988**, 111, 431.
- [42] V. A. Efremov, E. N. Gudinitza, I. Matschek, A. A. Fakeev, *Zh. Neorg. Khim.* **1983**, 28, 1725.
- [43] R. Kniep, D. Koch, Th. Hartmann, *Z. Kristallogr. NCS* **2002**, 217, 186.